Noise and Bandwidth Performance of Single-Molecule Biosensors

J. Rosenstein, S. Sorgenfrei, K. L. Shepard
Bioelectronic Systems Laboratory, Columbia University, New York, NY

***Abstract*— Technological advances in fluorescent probes, solid-state imagers, and microscopy techniques have enabled biomolecular studies at the single-molecule level. Fluorescent techniques are highly specific but their bandwidth is fundamentally limited by the number of photons that can be collected. New electronic sensors including nanopores and nanotube field-effect transistors offer different tradeoffs between bandwidth and noise levels. Here, we discuss the performance of these direct solid-state interfaces and their potential for sensing single-molecule dynamics at shorter timescales.**

I. Introduction

Biomolecular systems are traditionally studied using fluorescence-based ensemble measurements of the average characteristics of a relatively large number of molecules. Among the most common *in vitro* applications are DNA microarrays to identify gene expression profiles [1] and enzyme-linked immunosorbent assays (ELISA) to identify proteins [2]. While much can be determined with ensemble measurements, scientific and technological interest is rapidly moving to single-molecule techniques. When probing biomolecules at the single-molecule level, dynamics can be observed which are usually hidden in ensemble measurements. The most popular single-molecule techniques are also based on fluorescence [3]. Though fluorescent probes are highly specific, they use light as an intermediary between the biological system and measurement electronics, which results in fundamental constraints in resolution and bandwidth due to the countable number of photons emitted. Single-molecule measurements of the kinetics of fast biomolecular processes are often unavailable through fluorescent techniques, as they lack the necessary temporal resolution.

Alternative non-optical single-molecule techniques have been developed based on force spectroscopy, such as optical tweezers [4] and atomic force microscopy [5]. New electrochemical methods are also being explored which provide higher bandwidth measurements. Nanopores represent one such technique, in which a single molecule is measured as it passes through a nanoscale pore in a thin membrane [6]. Another recent technique attaches a probe molecule directly to a defect in a carbon nanotube, creating a highly-sensitive field effect transistor which responds to the presence of individual target molecules [7]. By providing direct interfaces to solid-state electronics, both nanopore and nanotube sensors can achieve higher detection bandwidth than fluorescence-based approaches, at the expense of higher background noise and interference levels.

In this paper, we will further explore the nature of direct solid-state interfaces to biomolecular systems by examining both nanopore and field-effect sensors, and contrasting their performance with fluorescence-based approaches. In Section II, we consider the overall signal chain for biomolecular sensing systems, including the interface to solid-state electronics. In Section III, we describe and compare three representative single-molecule sensing systems based on fluorescence, nanopores, and field-effect sensors. Section IV concludes.

II. Biomolecular Sensing Systems

A. Overview

At its most fundamental level, the task of any sensor is to infer the internal state of a system through a set of external observations. Due to the limited signal levels available from single molecules, a compromise is often made to observe only discrete states such as the presence or absence of a molecule or discrete conformational changes in a single molecule. Any real sensor will have some degree of variability in its output, leading to uncertainty in estimates of the system's state. We can refer to all of this uncertainty as measurement noise, but it is instructive to categorize the paths through which noise can appear in a measurement.

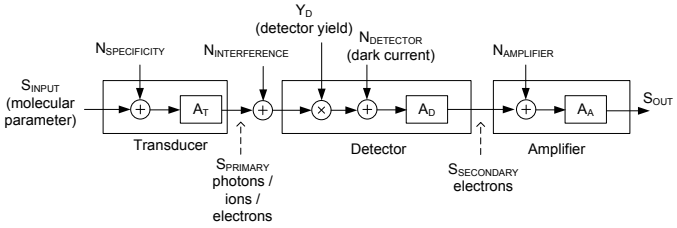

Figure 1. System block diagram

A conceptual schematic of a biosensor signal path is shown in Fig. 1. The system is separated into a transducer, detector, and amplifier. The transducer interfaces directly to the biomolecule and produces a set of signals which correspond to the presence (or state) of an analyte molecule. The output of the transducer may take the form of photons, ions, or electrons depending on the transducer. The detector converts the transducer output into an electrical current. An amplifier adjusts the signal level such that it is appropriate to interface with other electronic circuits and data converters.

The absence of extraneous signals that influence the transducer by the same means as the analyte molecules

978-1-4577-0223-5/11/$26.00 ©2011 IEEE

describes the 'specificity' of a sensor. This category of noise can include effects such as nonspecific adsorption to the sensing area, or the degree to which a transducer produces a similar signal from other molecules in the solution.

In contrast to signals that originate at the sensor input, when unwanted signals arrive later in the signal chain they are uncorrelated with the transducer output and are categorized as part of the background detection level. These effects include such effects as the dark current of a photodetector, or noise added from an amplification stage.

It is useful to refer the contribution of any measurement noise back to the input of the system. This is done by divided the noise by the total gain to that point in the signal chain. In this way, a high-gain transducer can reduce the contributions of noise which appears later in the signal chain.

The input-referred noise power (N_{INPUT}) of the general system of Fig. 1 is given by:

$$N_{INPUT} = N_{SPECIFICITY} + \frac{N_{INTERFERENCE}}{A_T{}^2} + \frac{N_{DETECTOR}}{(Y_D A_T)^2} + \frac{N_{AMPLIFIER}}{(A_D Y_D A_T)^2} \qquad (1)$$

This formulation of the noise includes sources of noise and interference which exist throughout in the signal. However, we have thus far assumed that all of the signals are continuous quantities. For the weak signals produced by single-molecule biosensors this can be a poor assumption, as $S_{PRIMARY}$ may consist of a countable number of particles. As a result, when interrogating biomolecular processes which occur on millisecond- or microsecond-timescales, the signal presented to the detector can be extremely quantized both in time and amplitude.

In the context of weak discrete signals, it may not be immediately obvious how to specify the gain of the transducer, A_T. Traditionally we consider the gain to be a ratio of continuous amplitudes along a signal chain. But for signals made of discrete particles, we must instead think in terms of the rate of output signals, rather than their amplitude. For modeling purposes, we can imagine the transducer output to be a Poisson process which generates an average of N discrete observations per time τ. The expected rate of observations $\lambda^{-1}=N/\tau$ is the gain.

If the gain of the transducer is low then for short intervals, $E\{N\}$ is small and there is high variance in the measurements, which can be described as either thermal or shot noise, depending on the context [8]. This is intrinsic to working with weak quantized signals, rather than deriving from other competing fluctuations in the system. The impact of this noise decreases as the number of observations increase. In the limit of either high transducer gain or long measurement intervals, the system approaches a continuous output.

B. Signal-to-noise ratio and bandwidth

While evaluating different biosensing platforms, ideally one could compare their signal-to-noise ratios (SNR). However, as both the signal and noise of a sensor are functions of frequency, so too is the SNR. Given a particular signal and sensor, there will be a measurement bandwidth which optimizes the SNR. This optimal bandwidth is also a function of the characteristics of the input signal. In particular, if the noise spectrum is flat but the signal fluctuations are band-limited then increasing the bandwidth will improve the SNR until the bandwidth exceeds the frequency content of the signal.

Even for given input signal characteristics, the ideal operating bandwidth is a function of what parameters are being measured. A measurement of the average state of a single fluctuating molecule would be optimized with a lower bandwidth than a measurement of the molecule's kinetic parameters.

C. Properties of effective single-molecule sensing systems

Given this signal-chain perspective of single-molecule biosensors, before we consider particular example systems, it is interesting to generalize what features make for the best sensors.

To be able to make single-molecule measurements at all, one requires a system whose output is sensitive to a very small physical volume. If a transducer is sensitive to activity in a relatively large volume, it is very easy for background noise to overwhelm any single-molecule measurements. In optical systems this localization can be achieved with lenses and strategic illumination patterns. In electromechanical and electrochemical systems it is more a direct function of the dimensions of the sensor.

Even with its sensitivity physically localized, a sensor may respond to other molecules present in the sample. Specificity in single-molecule measurements is generally achieved by chemical selectivity, by using proteins or functional groups which specifically bind to the target molecule.

An ideal sensor will also have high gain, producing a high rate of observations of its sensing area. A high gain transducer can ease the impact of noise later in the signal chain, and can be leveraged either to increase the bandwidth of the system or to lower the minimum detectable signal.

III. REPRESENTATIVE SINGLE-MOLECULE SYSTEMS

A. Fluorescence-based systems

Over the last two decades fluorescent techniques have become the standard method for probing molecules at the single-molecule level both *in vivo* and *in vitro*. Förster resonance energy transfer (FRET) has been used to study interactions between nucleic acid molecules [9], protein folding [10] and particle tracking [11]. In this technique, the dipole-dipole interaction of a donor and acceptor fluorophore is used to obtain information about their spatial separation. The donor fluorophore's emission spectrum overlaps with the acceptor fluorophore's excitation spectrum, as depicted in Fig. 2. The donor fluorophore can transfer energy to the acceptor

fluorophore according to the following relationship for the fraction of energy transferred,

$$E = \frac{1}{1+\left(\frac{R}{R_0}\right)^6} \qquad (2)$$

where R is the distance separating the molecules and R_0 is the characteristic distance of the FRET pair (Fig. 3) [12]. This highly nonlinear relationship allows detection of the molecules' interactions at extremely small length scales.

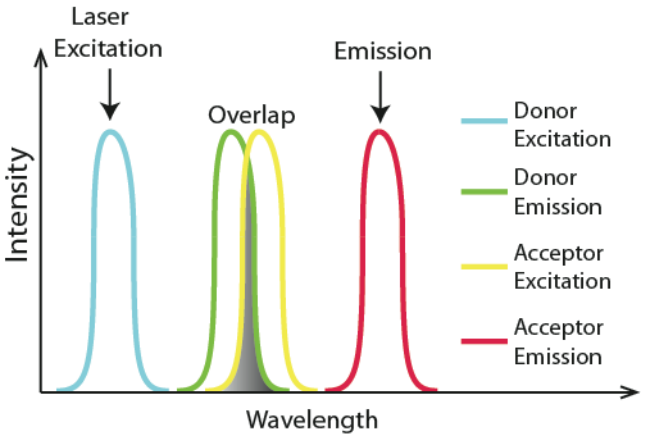

Figure 2. A schematic representation of the excitation and emission spectrum of a FRET pair.

In FRET experiments, the donor and acceptor fluorophore are attached to the biomolecules of interest and the donor and acceptor emission intensities are recorded. By recording the normalized intensity ratio, one can calculate the distance between the two molecules as a function of time and, therefore, monitor inter and intra-molecular binding, folding and conformation kinetics.

Modern optical microscopes and the availability of very low-noise photon detectors have improved the signal-to-noise ratio and driven FRET to single-molecule levels of sensitivity. In one common setup, probe molecules are tethered to the surface and total internal reflection (TIRF) microscopy is used to excite a thin volume at the surface of a sample. In other arrangements, molecules in solution are examined in a very small volume using confocal or two-photon microscopy. By confining the donor excitation energy to a very small volume these techniques produce extremely low background noise levels and allow highly specific detection of FRET interactions.

One of the biggest constraints in FRET measurements is that the fluorophores eventually photobleach, which limits the number of observations that can be made of a molecule. Depending on the power level of the excitation source, photobleaching either limits the total measurement time or the rate at which a FRET pair can be observed.

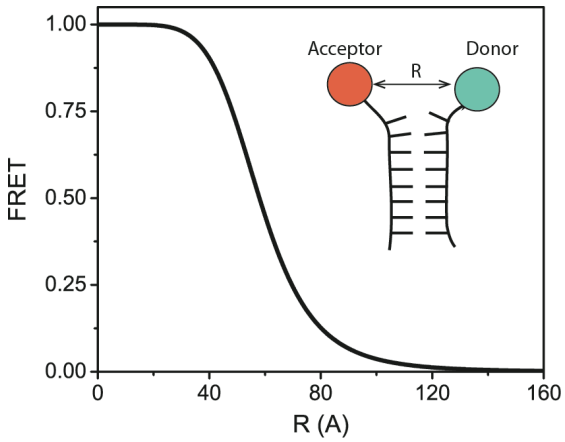

Figure 3. The ratio of FRET acceptor and donor fluorescent emission intensity as a function of their separation distance. (R_0=58Å)

B. *Nanopore systems*

A nanopore sensor is an electrochemical sensor consisting of a small aperture in a thin membrane [13], as shown in Fig. 4. The two sides of the membrane are exposed to two isolated fluid reservoirs, which are filled with an electrolyte solution. A voltage is applied between the reservoirs, resulting in a potential difference across the membrane, as well as across the nanopore. A baseline bias current can be measured which corresponds to the flux of dissolved ions moving from one reservoir to the other. Physically this arrangement is a direct equivalent to ion channels in biological membranes, which are in fact one way to construct such a sensor [13].

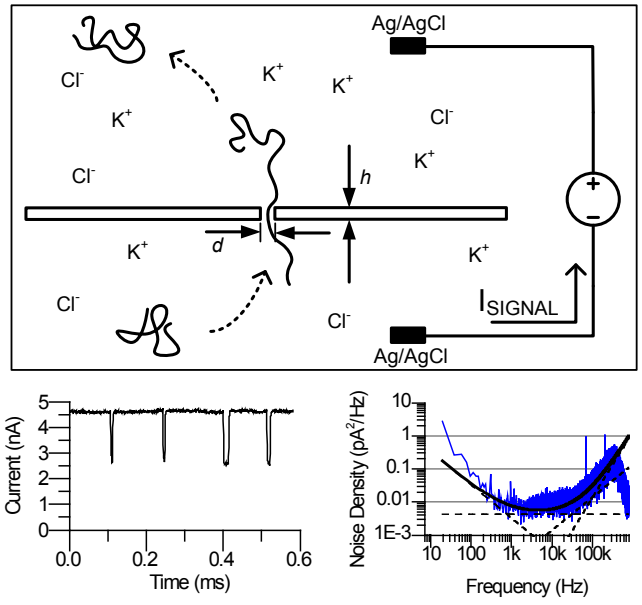

Figure 4. Nanopore sensor schematic representation. Insets: time domain DNA translocation events through a 3nm Si_3N_4 nanopore and measured noise spectrum

When other charged molecules such as DNA are introduced into the electrolyte, the electric field at the pore can also induce these molecules to translocate through the pore. The presence of a lower-mobility molecule in the pore alters its conductivity, and can be observed by a transient change in the measured current.

The ability of a nanopore sensor to produce a large output signal corresponding to a single molecule of DNA is a function of its nanoscale geometry. The diameter d of a pore can range from 2-10nm, and due to electrolyte charge screening the measured current is highly insensitive to charge sources more than a few nanometers from the pore. A simplified electrical model of a nanopore is to treat it as a resistive cylinder of diameter d and length h. The pore contains mobile charges in the form of dissolved ions with a volume concentration σ_{IONS} and mobility μ_{IONS}. By this model, the baseline bias current can be described by [14]:

$$I_{BIAS} \approx V_{BIAS}\sigma_{IONS}\mu_{IONS}\frac{\pi d^2}{4h} \qquad (3)$$

As a first-order approximation, we can assign a long molecule of DNA an effective length L_{DNA}, electrophoretic mobility μ_{DNA}, and electrostatic cross-sectional area A_{DNA} in which it excludes mobile ions. The mobility will result in a characteristic transit time τ and the presence of the molecule in the pore will result in a change in the measured ionic current. Together, this means the total number of unit charges collected per molecule is:

$$n_{SIGNAL} \approx \frac{\Delta I \times \tau}{q} \approx \sigma_{IONS} A_{DNA} \frac{1}{q}\frac{\mu_{IONS}}{\mu_{DNA}}\frac{L_{DNA}}{h} \qquad (4)$$

A nanopore provides gain through the effect that a comparatively slow-moving DNA molecule has on the nearby concentration of higher-mobility salt ions.

We note that the pore diameter d affects I_{BIAS} but not n_{SIGNAL}. As a result, d primarily affects the background signal level. If the pore is much larger than the effective cross-section of a translocating molecule, then the noise associated with the bias current can quickly obscure the signal. Typically the most sensitive nanopores have diameters of 3nm or less.

The finite thickness h of the membrane also diminishes the geometric sensitivity of the pore, and in the case of DNA translocations many bases will occupy the pore at one time. The membrane thickness also plays a role similar to the channel length of a transistor, with an inverse relationship between h and I_{BIAS}. Fabricating nanopore sensors in membranes such as graphene [15] and ultra-thin Si_3N_4 [16] produce gain and bandwidth improvements analogous to those achieved by FET channel length scaling.

Another aspect limiting the signal-to-noise level of nanopore sensors is the parasitic capacitance associated with coupling of the two reservoirs across the thin membrane. This capacitance interacts with the transimpedance amplifiers used to measure the sensors and causes an increase in noise density at high frequencies [17]. This in turn limits the practical measurement bandwidth to less than 100kHz.

C. *Field-effect sensors*

Field-effect transistors, in the form of carbon nanotube devices, can be used as highly sensitive biosensors, as shown in Fig. 5a. A cylindrical tube of carbon atoms with a diameter of approximately 1.5 nm is used as a channel. Source and drain electrodes are made from titanium and a silicon back gate with a 300 nm thermal oxide can be used to modulate the electron carrier density in the channel. For biological experiments, an electrolyte buffer with mobile ions can also be used to gate the transistor [18]. Early versions of this style of sensor attempted to detect molecules adsorbed onto pristine [19] and coated carbon nanotubes [20], but did not yield single molecule resolution. In this arrangement the lowest detection limit reported for DNA was 14 pM [19]. The sensing mechanism was attributed to both changes in the Schottky barrier at the contacts and electrostatic doping of the nanotube channel due to adsorption of biomolecules [21].

We have recently demonstrated that single-molecule sensitivity can be achieved by creating a defect in the carbon nanotube channel [22]. The nanotube is electrochemically oxidized, yielding a channel whose resistance is dominated by a single point along its length. We have used scanning gate microscopy to image the sensitivity of the nanotube before and after the oxidation by using a biased tip (-5V) of an atomic force microscope (Fig. 5b). Before oxidation, electron transport in the nanotube is sensitive both to the Schottky barrier of the lower electrode, and also to other points along the channel. After oxidation, the sensitivity is localized to a small region in the middle of the channel. A short chemical reaction with a strong oxidizer (potassium permanganate) ensures that the defect functional group is converted to a carboxylic acid to which we covalently attach a probe DNA molecule as a specific probe.

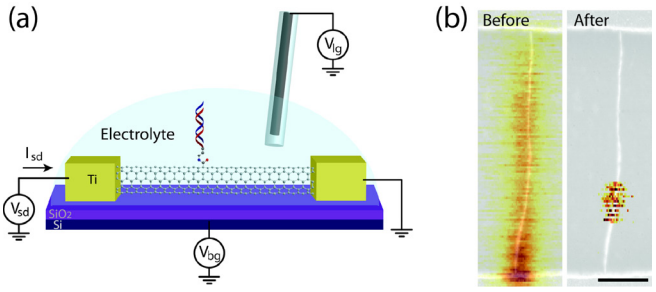

Figure 5. (a) Carbon nanotube FET system illustration and (b) scanning gate microscopy images before and after oxidation

As shown in Fig. 6, when the carbon nanotube is measured in 1X PBS buffer solution with a 10-mer oligonucleotide probe attached at the 5'end (NH2-5'-

GTGAGTTGTT-3'), the conductance has a single state which is dominated by flicker noise. After adding complementary ssDNA molecules to the solution, the conductance exhibits two level fluctuations as shown in Fig. 6. By studying the fluctuations as a function of temperature, we have correlated the high state in the conductance to the defect with probe only and the low state to a defect with duplex DNA. We can speculate that the negatively charged target DNA modulates a tunnel barrier at the defect site through electrostatic interaction or scattering and thereby reduces its conductance. In addition to the two-level fluctuations, there is also a small decrease in the overall conductance, which we attribute to non-specific adsorption of biomolecules to the sidewall of the nanotube.

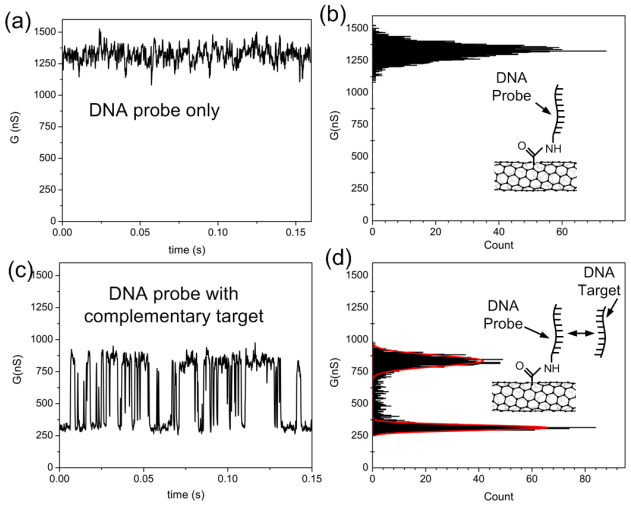

Figure 6. Carbon nanotube FET time-domain measurements showing the two-level response to single-molecule hybridizations

One of the advantages of using a carbon nanotube as a single-molecule sensor is that the small defect allows both spatial confinement through the small defect size and also a comparatively high transconductance. Currently prototype devices have large parasitics, limiting the bandwidth to less than 10kHz. The parasitics can be greatly reduced by improved device geometry and further system integration. Also because the corner frequency of the 1/f noise exceeds 10MHz, there is only a small decrease in the SNR by going to higher bandwidths, making the device ideal for sensing fast molecular interactions.

D. Comparison and discussion

Despite their significant differences it is worthwhile to find general metrics by which to compare these optical and electrochemical sensing approaches. An exact comparison will depend strongly on the specifics of each sensor. We have summarized some parameters relevant for comparison in Table I.

TABLE I. COMPARISON OF THE SENSORS

	Fluorophore	*Nanopore*	*CNT FET*
Spatial sensitivity	Rayleigh limit (~200nm)	Pore diameter (~5nm) and length (<50nm)	Defect size (<10nm) / Debye length
Transducer gain	Low	Moderate	High
Specificity	High	Low	Moderate
Transducer Output	Photons	Dissolved ions	Electrons
Detector	Photodiode / PMT / SPAD	Ag/AgCl electrode	None
Dominant noise	Shot noise	Flicker noise Thermal noise	Flicker noise Shot noise
Signals per nucleotide	10,000 (Cy5) 100 million (QD)	1,000	10 million
Signals per second	2,500 (Cy5) 500,000 (QD)	6 billion	100 billion

The ability to distinguish multiple fluorescent probes is commonly diffraction-limited to separations on the order of 200nm [23]. This is relatively large in comparison to the geometry of a nanopore or the defect size of a carbon nanotube FET, even after taking into account the effects of electrochemical Debye screening. However, some FRET techniques can take advantage of the highly localized resonant energy transfer distances to identify sub-nanometer differences in the relative positions of the donor and acceptor [12].

The specificity of proteins and functional groups used in fluorescent imaging techniques can be extremely high. Nanotube FETs could conceivably achieve similar specificity with appropriate probe molecules, but may be constrained to smaller molecules by Debye screening lengths. Non-specific adsorption to areas of the nanotube aside from the functionalized defect can also reduce the specificity. Nanopores usually have relatively little chemical selectivity, instead distinguishing molecules primarily based on their geometries and net electrical charges.

The effective gain of the three sensors differs by several orders of magnitude. Fluorophores' emission rates depend on their excitation power, but for a point of comparison we might use a typical number of 2,500 photons per second [23]. Inorganic fluorophores such as quantum dots can tolerate higher excitation levels and be far brighter, producing upwards of several hundred thousand photons per second. Neither of these optical techniques, however, come close to the gain of either of the electrochemical sensors. Solid-state nanopores can produce ionic current signals from single molecules in the low nanoampere range, corresponding to several billion ions per second. The gain of carbon nanotube FETs is even higher, as a function of their direct transduction to a channel of electrons, which have very low mass and, therefore, very high mobility compared to ions in a buffer solution.

Another perspective on the gain of the three transducers is to consider how many signals are produced per molecule of

analyte. Generally even single-molecule sensors are used to produce ensemble statistics of a population of molecules, by assembling the observations of many distinct molecules. Conceptually, the number of observations made on each molecule can correlate to the degree of subtle differences one might observe within the population. Fluorescent probes are fundamentally limited by photobleaching, yielding as few as 10,000 photons for organic dyes. Nanopore sensors are limited by the transient nature of their signals; though they have very high gain, they can only interrogate each molecule for the short period of time it occupies the pore. Long DNA molecules may take several milliseconds to translocate, corresponding to millions of ions per molecule, but normalized to the length of the polymer the signal is closer to a mere 1,000 ions per nucleotide. Carbon nanotube FETs combine their high gain with somewhat longer dwell times than nanopores, producing millions of electrons of signal from each small molecule temporarily captured by the probe.

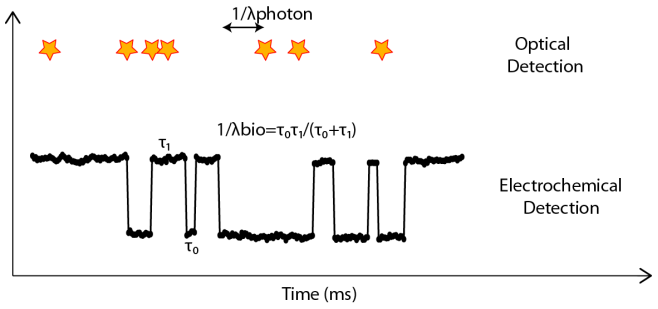

Figure 7. An illustration of the comparative timescales of the outputs of optical and electrochemical sensors

The different transducer output signals and effective gains result in different elements of the signal chain dominating the signal-to-noise performance in each sensor. Optical sensors have the benefit of very high specificity and very high-gain photon detectors. Therefore, they are constrained at low frequencies by the detector's dark current and at high frequencies by the shot noise of the weak signal. Nanopores have flicker noise which dominates at low frequencies, and at high frequencies they are limited by electrical parasitics and amplifier noise. Nanotube FETs are nearly entirely limited by flicker noise, but at high frequencies they can also run into electrical noise from parasitic impedances and amplifier noise.

E. Model system simulations

Clearly there will be a tradeoff between optical and electrochemical sensors in terms of specificity and gain. This results in different trends in the signal-to-noise ratio as a function of bandwidth. To compare the two, we imagine that they are each utilized to observe a Poisson process (Fig. 7). A single molecule fluctuates randomly between two states at an average rate of λ_{BIO} times per second, which is varied from 1Hz to 1MHz. An optical system is assumed to produce λ_{PHOTON}=5,000 photons per second, regardless of λ_{BIO}, and a nanotube FET is assumed to produce a 10nA signal current. For the optical system we assume that we have an ideal photon detector with zero dark count. The electrochemical sensor is given a flicker noise component which dominates its noise spectrum, and a signal roll-off beginning at 10kHz due to electronic parasitics. For each system we assume the sensor to be followed by a matched filter corresponding to the Lorentzian spectral content of the fluctuations.

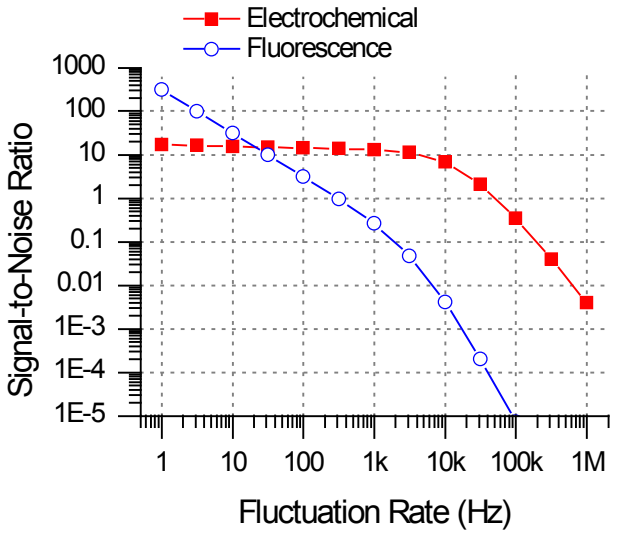

Figure 8. Simulated SNR of transient two-level fluctuations as observed by a FRET pair versus a carbon nanotube FET sensor

The results of these models are shown in Fig. 8. This plot shows the SNR as a function of the average rate of molecular fluctuations. We define the SNR as the ratio of the total signal power to the total noise power after the matched filter.

Clearly different trends exist in the two systems. The optical system has a flat shot noise spectrum, and as a result its SNR decreases steadily with bandwidth. The nanotube sensor, in contrast, exhibits 1/f noise which dominates at low fluctuation rates, yielding an SNR which is relatively insensitive to bandwidth. The absolute value of this flicker noise is a function of the nanotube's length [24], suggesting that SNR could be further improved by fabricating shorter devices. The SNR begins to decrease more rapidly after the transducer bandwidth is exceeded.

IV. CONCLUSIONS

Studying single-molecule dynamics requires transducers and signal chains with extremely high specificity and low background noise. Fluorescent techniques fulfill these requirements at the expense of low photon counts, which directly limit the signal bandwidth. Development will continue on brighter dyes and advanced microscopy techniques, which will improve the bandwidth available to fluorescent systems.

In contrast, electrochemical sensors have adequate gain but have historically been limited by background noise and

nonspecificity. Advances in nanotechnology have provided new materials and fabrication techniques that allow the fabrication of devices which approach the dimensions of single molecules. This has opened the door to new high-bandwidth sensing technologies based on direct charge detection and solid-state sensors. In the case of nanopore sensors, improvements in pore fabrication, surface chemistry, and reductions in electrical parasitics provides a path for lower noise levels. For single-molecule field-effect sensors, engineering devices with shorter channel lengths and lower parasitics should provide significant bandwidth improvements.

Whereas photons provide a conveniently discrete boundary between the transducer and detector electronics, single-molecule electrochemical sensors require a tighter integration of the transducer and signal amplification. This motivates strong cooperation between biochemical and electronic engineering efforts, as it requires a combined understanding of biophysics and solid-state electronics to optimize the sensor performance.

V. ACKNOWLEDGEMENTS

This work was supported in part by the National Institutes of Health under Grant R33-HG003089 and by the National Science Foundation under Grant ENG-0707748. Additional support was provided by the Focus Center Research Program through the Center for Circuit and System Solutions (C2S2) and the Office of Naval Research under Grants N00014-09-01-0250 and N00014-09-1-1117

REFERENCES

[1] M. Schena, *et al.*, "Qualitative Monitoring of Gene Expression Patterns with a Complementary DNA Microarray," *Science,* vol. 270, pp. 467-470, Oct 1995.

[2] E. Engvall and P. Perlmann, "Enzyme-Linked Immunosorbent Assay, Elisa," *The Journal of Immunology,* vol. 109, pp. 129-135, July 1, 1972 1972.

[3] E. A. Jares-Erijman and T. M. Jovin, "FRET imaging," *Nature Biotechnology,* vol. 21, pp. 1387-1395, 2003.

[4] A. D. Mehta, *et al.*, "Single-Molecule Biomechanics with Optical Methods," *Science,* vol. 283, pp. 1689-1695, March 12, 1999 1999.

[5] M. Carrion-Vazquez, *et al.*, "Mechanical design of proteins studied by single-molecule force spectroscopy and protein engineering," *Progress in Biophysics and Molecular Biology,* vol. 74, pp. 63-91.

[6] C. Dekker, "Solid-state nanopores," *Nature Nanotechnology,* vol. 2, pp. 209-215, 2007.

[7] B. R. Goldsmith, *et al.*, "Conductance-Controlled Point Functionalization of Single-Walled Carbon Nanotubes," *Science,* vol. 315, pp. 77-81, Jan 2007.

[8] R. Sarpeshkar, *et al.*, "White noise in MOS transistors and resistors," *IEEE Circuits and Devices Magazine,* vol. 9, pp. 23-29, Nov 1993.

[9] M. I. Wallace, *et al.*, "Non-Arrhenius kinetics for the loop closure of a DNA hairpin," *Proc Natl Acad Sci U S A,* vol. 98, pp. 5584-9, May 8 2001.

[10] J. Fei, *et al.*, "Coupling of ribosomal L1 stalk and tRNA dynamics during translation elongation," *Mol Cell,* vol. 30, pp. 348-59, May 9 2008.

[11] Y. M. Wang, *et al.*, "Single molecule measurements of repressor protein 1D diffusion on DNA," *Physical Review Letters,* vol. 97, Jul 2006.

[12] C. Joo, *et al.*, "Advances in single-molecule fluorescence methods for molecular biology," *Annual Review of Biochemistry,* vol. 77, pp. 51-76, 2008.

[13] D. Branton, *et al.*, "The potential and challenges of nanopore sequencing," *Nature Biotechnology,* vol. 26, pp. 1146-1153, Oct 2008.

[14] R. M. M. Smeets, *et al.*, "Salt dependence of ion transport and DNA translocation through solid-state nanopores," *Nano Letters,* vol. 6, pp. 89-95, Jan 2006.

[15] C. A. Merchant, *et al.*, "DNA Translocation through Graphene Nanopores," *Nano Letters,* vol. 10, pp. 2915-2921, Aug 2010.

[16] M. Wanunu, *et al.*, "Rapid electronic detection of probe-specific microRNAs using thin nanopore sensors," *Nature Nanotechnology,* vol. 5, pp. 807-814, Nov 2010.

[17] R. M. M. Smeets, *et al.*, "Noise in solid-state nanopores," *Proc Natl Acad Sci U S A,* vol. 105, pp. 417-421, Jan 15 2008.

[18] S. Rosenblatt, *et al.*, "High performance electrolyte gated carbon nanotube transistors," *Nano Letters,* vol. 2, pp. 869-872, Aug 2002.

[19] A. Star, *et al.*, "Label-free detection of DNA hybridization using carbon nanotube network field-effect transistors," *Proc Natl Acad Sci U S A,* vol. 103, pp. 921-6, Jan 24 2006.

[20] K. Besteman, *et al.*, "Enzyme-coated carbon nanotubes as single-molecule biosensors," *Nano Letters,* vol. 3, pp. 727-730, Jun 2003.

[21] I. Heller, *et al.*, "Identifying the mechanism of biosensing with carbon nanotube transistors," *Nano Letters,* vol. 8, pp. 591-5, Feb 2008.

[22] S. Sorgenfrei, *et al.*, "Label-free single-molecule detection of DNA-hybridization kinetics with a carbon nanotube field-effect transistor," *Nature Nanotechnology,* vol. 6, pp. 125-131, Feb 2011.

[23] S. Ram, *et al.*, "Beyond Rayleigh's criterion: A resolution measure with application to single-molecule microscopy," *Proc Natl Acad Sci U S A,* vol. 103, pp. 4457-4462, Mar 21 2006.

[24] J. Mannik, *et al.*, "Charge noise in liquid-gated single-wall carbon nanotube transistors," *Nano Letters,* vol. 8, pp. 685-8, Feb 2008.